Cocontinuous Phase Morphology for an Asymmetric Composition of Polypropylene/Polyamide 6 Blend by Melt Mixing of Polypropylene with Premelted Polyamide 6/Organoclay Masterbatch

Li Wang, Zhao-Xia Guo, Jian Yu

Department of Chemical Engineering, Key Laboratory of Advanced Materials (MOE), Tsinghua University, Beijing 100084, People's Republic of China

Received 3 August 2010; accepted 30 March 2011
DOI 10.1002/app.34600
Published online 12 August 2011 in Wiley Online Library (wileyonlinelibrary.com).

ABSTRACT: Cocontinuous morphology was obtained for an asymmetric composition of polypropylene/polyamide 6 (70/30 w/w) blend by controlling melt compounding sequence of PP, PA6, and organoclay. Three different compounding sequences were tested: direct melt mixing of all the components, melt mixing of PP with PA6/organoclay masterbatch, and melt mixing of PP with premelted PA6/organoclay masterbatch. Only the third method promotes cocontinuous morphology. In all three cases, organoclay locates preferentially in the PA6 phase and at the interface, although the level of organoclay dispersion is poorer in the case of direct mixing than in the two-masterbatch approaches. The morphology evolution processes of the three different compounding sequences were investigated and revealed that the main reason for the formation of cocontinuous morphology in the third method is the inhibiting effect of organoclay preincluded in the premelted PA6 phase on phase inversion. The viscosity of PA6 phase and the barrier effect of organoclay were confirmed to be two key factors in promoting cocontinuous structure. Dynamic mechanical analysis shows that the blend having cocontinuous morphology displays higher storage modulus than those having matrix-dispersed morphology at the same organoclay loading. J Appl Polym Sci 123: 1218–1226, 2012

Key words: blends; clay; morphology; cocontinuous; sequence

INTRODUCTION

Blending of polymers is a common way of developing new materials, because it can bring about a combination of the advantages of different polymers. However, due to large unfavorable mixing enthalpy, most polymers are thermodynamically immiscible with each other and undergo phase separation during blending process. Generally, there are two major types of phase morphology for polymer blends: matrix-dispersed structure and cocontinuous structure. It is believed that cocontinuous morphology can only be obtained in a narrow composition region near phase inversion point, governed by the viscosity ratio between components.[1]

$$\frac{\varphi_1}{\varphi_2} = \frac{\eta_1}{\eta_2}, \quad (1)$$

where φ_i and η_i are the volume fraction and viscosity of the component i. Beyond this region, matrix-dispersed morphology is formed, with major component constituting continuous phase or matrix, while minor component existing in the form of dispersed domains. Although many useful polymer blends have matrix-dispersed morphology, obtaining cocontinuous structure from asymmetric compositions is gaining increasing attention in recent years[2–15] because the cocontinuous morphology can offer a better combination of the properties of each blend component.[9–15]

With the development of polymer/clay nanocomposites, clay was found to have significant effect on the phase morphology of polymer blends. For asymmetric compositions, the addition of clay can cause either a reduction or an increase in average dispersed domain size, depending on the dispersion and distribution states of clay.[16–25] In recent years, several research groups[5–14] have revealed that clay can promote the formation of cocontinuous morphology. Li et al.[6] reported the formation of cocontinuous morphology for PA6/PPO blends (50/50 w/w) by adding 5 wt % of clay. This was partly attributed to the selective distribution of clay in PA6 (major phase), which caused a dramatic decrease in viscosity ratio (η_{PPO}/η_{PA6}) and shifted the phase inversion point closer to the volume ratio used in

Correspondence to: Z.-X. Guo (guozx@mail.tsinghua.edu.cn) or J. Yu (yujian03@mail.tsinghua.edu.cn).

blending. Li et al.[9] also reported cocontinuous morphology for ABS/PA6 blends (60/40 w/w) by adding 2 wt % of clay. Wu et al.[7] discovered that cocontinuous morphology could be achieved in PE/PBT blends (60/40 w/w) when the amount of clay was over 2 wt %. Ray et al.[8] observed that 5 wt % of clay promoted cocontinuous morphology for PP/PBSA blends (80/20 w/w). A common feature of the last three examples (Refs. 7–9) is the preferential distribution of clay in the minor phase, causing its viscosity to increase. According to eq. (1), an increase in the viscosity of the minor phase shifts the phase inversion point farther from the volume ratio used in blending. Thus, eq. (1) fails to explain the formation of cocontinuous morphology.[10] The barrier effect of clay and the highly elongated domains resulted from the enrichment of clay were separately proposed by some researchers[9,10] as possible reasons for the formation of cocontinuous morphology by the incorporation of clay. It is noted that all the above-mentioned examples (Refs. 6–10) use direct melt mixing, a recent article[5] reported that preincluding organoclay in the minor phase can promote cocontinuous morphology when direct melt mixing fails, revealing the importance of compounding sequence in the formation of cocontinuous morphology.

PP/PA6 blend is a typical system of both research interest and industrial value. There have been some research on clay-filled PP/PA6 blends,[26–33] focusing on morphology, rheology, mechanical properties, crystallization behavior, and so forth. However, cocontinuous morphology has not been reported for asymmetric compositions of PP/PA6 blends by incorporation of clay. In this article, we aim at evaluating the possibility of using organoclay in promoting cocontinuous morphology for an asymmetric composition of PP/PA6 blend (70/30 w/w) and the effect of the morphological change on mechanical properties. Three different compounding sequences were tested, and only one gave cocontinuous morphology. The morphology evolution processes were investigated to know the formation mechanism of cocontinuous morphology. The contribution of the two important factors (viscosity ratio change and the barrier effect of clay) was verified by specially designed experiments. Dynamic mechanical analysis (DMA) was used to evaluate the mechanical properties of the blends.

EXPERIMENTAL

Materials

PP used in this study was a commercial product (S1003) of Yanshan Petroleum and Chemical (Beijing, China) PA6 (B3S) was purchased from BASF (Malaysia).

TABLE I
Designations and Compositions

Designation	Composition		
	PP	PA6	Organoclay
PA6–30–0d	70	30	0
PA6–30–0mi	70	30	0
PA6–30–5d	70	30	1.58
PA6–30–5md	70	30	1.58
PA6–30–5mi	70	30	1.58
PA6–30–2.5mi	70	30	0.77
PA6–30–10mi	70	30	3.33
PA6–20–5mi	80	20	1.05
PA6–20–10mi	80	20	2.22
PA6–20–15mi	80	20	3.53

The clay used was an organoclay supplied by Huate Group (Lin'an, China) under the trade name of NB901. It was a montmorillonite organically modified with a quaternary ammonium salt (CEC: 95 meq/100 g).

Sample preparation

Organoclay-filled PP/PA6 blends were prepared using a torque rheometer (RM200A, Harbin Hapro Electrical Technology). The screw speed, mixing temperature and mixing time were set to 60 rpm, 230°C and 10 min, respectively. Three mixing methods were used. In Method 1, all components were added to the mixer simultaneously, and thus denoted as "d," meaning direct melt mixing. Methods 2 and 3 are both PA6/organoclay masterbatch approaches. In Method 2, PP was added to the mixer along with the masterbatch pellets; while in Method 3, PP was added after the masterbatch pellets had been melted. Thus, Method 2 is denoted as "md," where "m" means masterbatch approach, "d" means direct mixing PP with the masterbatch; Method 3 is denoted as "mi," where "i" means intermediate feeding of PP. The designations and compositions of all samples are given in Table I. For example, PA6-30-5mi means that the method used is "mi" and the PA6 content is 30 wt% (to all polymers) with 5 wt % of organoclay (to PA6), correspondingly to 1.58 phr.

Separation of PA6 phase

PA6 phase was separated by Soxhlet extraction with xylene for 48 h to remove PP phase completely.

Characterization

Field emission scanning electron microscopy (FESEM)

FESEM observation was conducted on a JEOL JSM-7401F apparatus operating at an accelerating voltage

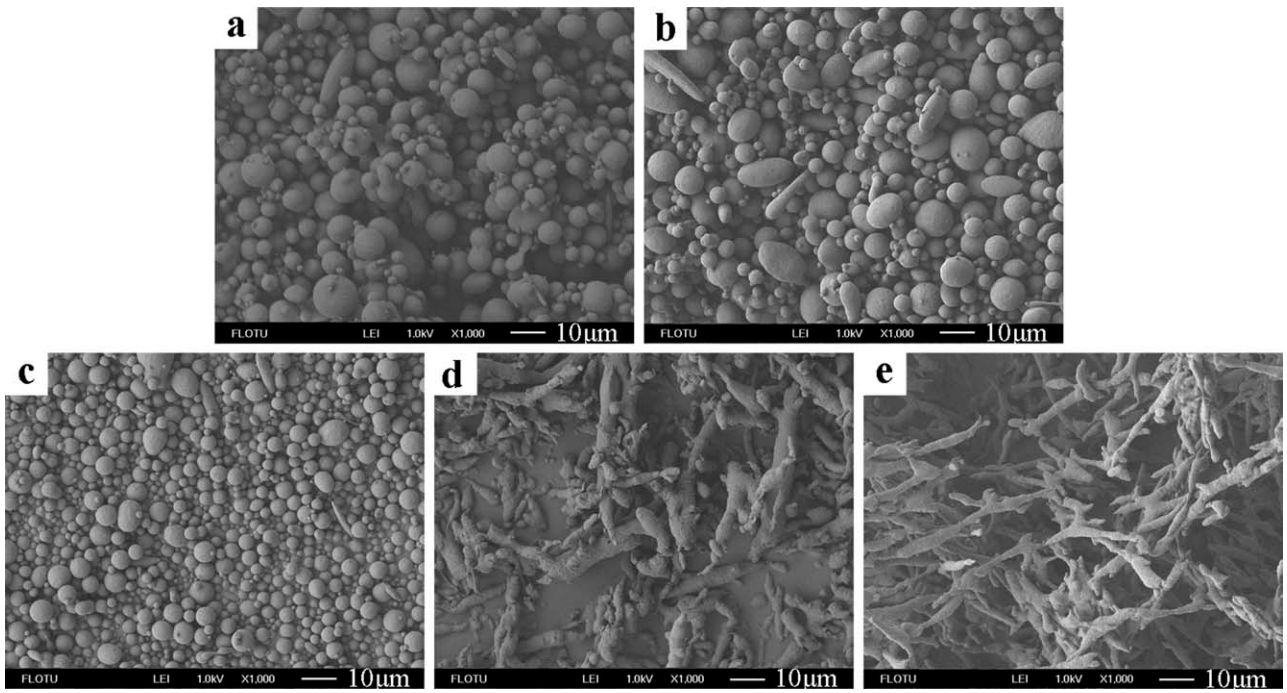

Figure 1 FESEM images of the PA6 phases of PP/PA6 blends without and with 5 wt % of organoclay (relative to PA6) prepared by different compounding sequences: (a) PA6-30-0d, (b) PA6-30-0mi, (c) PA6-30-5d, (d) PA6-30-5md, and (e) PA6-30-5mi.

of 1 kV. A JEOL software (SMILEVIEW) was used to measure the size of the PA6 phase.

X-ray diffraction (XRD)

X-ray diffraction was performed using a Rigaku D/max-RB diffractometer operating at 40 kV and 200 mA. The beam used was Cu Kα radiation with a wavelength of 1.5418 Å. Data were collected in the range from 1.5° to 10° at a scanning rate of 1°/min.

Transmission electron microscopy (TEM)

TEM observation was operated on a Hitachi H-800 transmission electron microscope at an accelerating voltage of 200 kV. Ultrathin slices were obtained using a cryo-ultratome (LKB model 2088; LKB-Producter AB, Bromma, Sweden) without staining.

Melt flow index (MFI)

MFI of PA6/organoclay with different organoclay loadings was measured by a Gotech melt flow indexer (GT-7100-MI). The temperature was set at 230°C and a load of 1 kg was used.

Equilibrium torque

Equilibrium torque of PA6/organoclay with different organoclay loadings was obtained from the torque rheometer to evaluate the influence of organoclay addition on the viscosity of PA6 phase.

Dynamic mechanical analysis (DMA)

All tested samples were hot-compressed into thin films at 190°C, which was below the melting point of PA6 to prevent change in morphology. DMA was performed in a temperature range of −100–150°C at a heating rate of 5°C/min, using a Dynamic mechanical analyzer 2980 (TA Instruments). The frequency was 1 Hz and the strain was 20 μm.

RESULTS AND DISCUSSION

Effect of compounding sequences

To investigate the conditions for the formation of cocontinuous morphology, three different compounding sequences were used and compared: direct melt mixing (d), masterbatch approach with direct addition of PP (md), and masterbatch approach with intermediate feeding of PP (mi). FESEM observation of the isolated PA6 phases was used to investigate the phase morphology of the PP/PA6 blends, because the cryofractured surfaces of the blends could not give a clear reveal of the cocontinuous phase morphology when PA6 phase appears as elongated network structure.[34] The images are shown in Figure 1. For samples without organoclay (PA6-30-0 d and PA6-30-0mi), typical matrix-dispersed morphology was formed, with most dispersed domains being spherical. The average particle diameters are 4.5 and 4.3 μm for

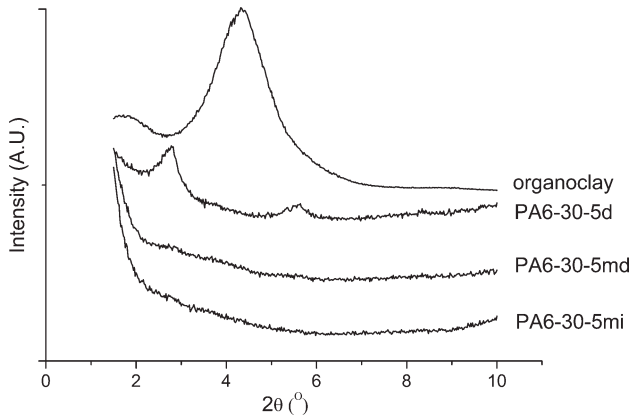

Figure 2 XRD patterns of organoclay and PP/PA6 blends with 5 wt % of organoclay prepared by different compounding sequences.

PA6-30-0d and PA6-30-0mi, respectively, indicating that the compounding sequence has almost no influence on phase morphology when clay was not used. However, great differences were observed among samples with 5 wt % of organoclay, to PA6, (PA6-30-5d, PA6-30-5md and PA6-30-5mi). The phase morphology of PA6-30-5d resembles that of PA6-30-0d and PA6-30-0mi, except that the average particle diameter is much smaller (3.1 μm) due to the barrier effect of organoclay. For sample PA6-30-5md [Fig. 1(d)], although matrix-dispersed type morphology is obtained, the shape of dispersed domains changes significantly, a mixture of rod-like, branched, and irregular structure was observed. For sample PA6-30-5mi [Fig. 1(e)], the elongated network structure of the PA6 phase was observed, suggesting the formation of cocontinuous structure. The average fiber diameter constituting the network structure is $\sim$ 2.5 μm. This is in agreement with what has been reported in Refs. 27,32, and 33, in which direct mixing and mixing PP, with premixed PA6/organoclay, yielded matrix-dispersed type morphology. Because the aim of this work is to investigate the conditions for the formation of cocontinuous morphology, only mi sequence was used in the investigation of other parameters.

The XRD patterns of organoclay and all samples containing 5 wt % of organoclay are given in Figure 2. Pristine organoclay exhibits a broad peak at $2\theta = 4.32^\circ$, corresponding to a gallery distance (d) of 2.05 nm. For sample PA6-30-5d, the diffraction peak of organoclay is shifted to $2\theta = 2.78^\circ$ ($d = 3.18$ nm), indicating that only intercalated state of organoclay was achieved. For sample PA6-30-5md and PA6-30-5mi, no obvious peak was observed, indicating that at least partial exfoliation of organoclay was reached.

TEM observation was conducted to gain an intuitive insight into the distribution and dispersion states of organoclay for all samples containing 5 wt % of organoclay and the images are shown in Figure 3. It is not difficult to distinguish the PP phase from the PA6 phase because PP is the major component in the blends (about 75% in volume). It can be seen that no matter which blending sequence is used, organoclay locates preferentially in the PA6 phase and at the interface. This is in agreement with the results of Su et al.[33] for PP/PA6 blends prepared by one-step mixing using an internal mixer. However, the dispersion state of organoclay in sample PA6-30-5d is different from that in the other two samples. Large aggregates and intercalated structure of organoclay were observed in sample PA6-30-5d, while intercalated structure of organoclay and thin lines representing exfoliated platelets were observed for the other two samples. These are consistent with the results of XRD.

Morphology evolution processes in different compounding sequences

The morphology evolution process was considered to understand the dramatic distinction in phase morphology resulted from different compounding sequences. Thus, a small amount of the melt was taken from the chamber of torque rheometer at different time intervals (2, 4, and 7 min) and immersed

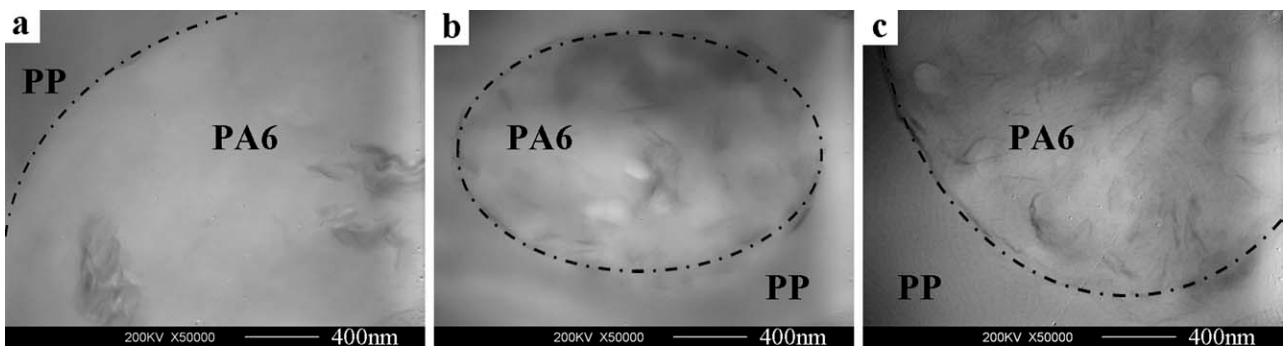

Figure 3 TEM images of PP/PA6 blends with 5 wt % of organoclay prepared by different compounding sequences: (a) PA6-30-5d, (b) PA6-30-5md, and (c) PA6-30-5mi.

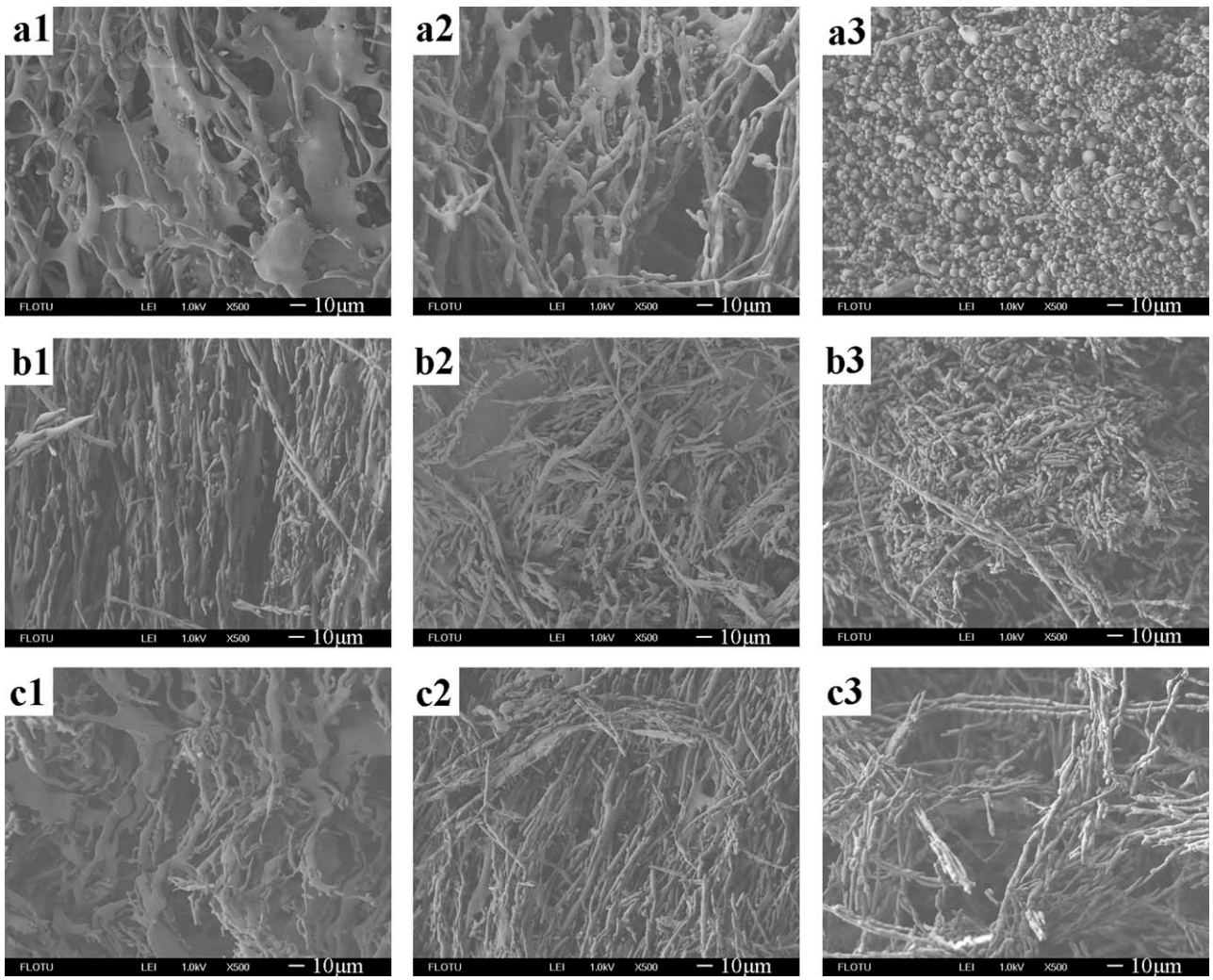

Figure 4 Morphology evolution processes in different compounding sequences as illustrated by the isolated PA6 phases after 2, 4, and 7 min of mixing: (a1–a3) PA6-30-5d, (b1–b3) PA6-30-5md, and (c1-c3) PA6-30-5mi.

into cold water quickly to freeze the morphology, then extracted with xylene to remove the PP phase. The isolated PA6 phases were observed by FESEM.

It has been reported by Scott and Macosko[35] that the initial stage of polymer blending involves the formation of sheets or ribbons from dispersed polymer pellets and then a two-dimensional network of dispersed phase due to interfacial instabilities. If the two-dimensional network cannot endure Rayleigh-type instabilities during further blending, it breaks up into irregular shaped particles and finally nearly spherical particles were observed due to shape relaxation. During the compounding process of PA6-30-5d and PA6-30-5md, PP melted before PA6 because of its relatively lower melting temperature, and PA6 or PA6/5 wt % organoclay pellets got dispersed in the PP phase. Thus a two-dimensional network of the PA6 phase was formed at the initial stage [Fig. 4(a1,b1)]. For PA6-30-5d, organoclay entered into the PP phase after PP had melted and it took time for organoclay to migrate to the interface and PA6 phase,[33] and therefore organoclay was not beneficial to the preservation of the PA6 network, and breakup process gradually took place [Fig. 4(a2)], yielding spherical particles eventually [Fig. 4(a3)]. For PA6-30-5md, although the preinclusion of organoclay in the PA6 phase decreases the ability of the PA6 phase to deform and break up, the PA6 network still could not endure large extension in flow field and breakup took place [Fig. 4(b2,b3)]. Because the presence of organoclay in PA6 hindered the shape relaxation of the dispersed domains to spherical particles, a mixture of rod-like, branched, and irregular structure was obtained. In the case of PA6-30-5mi, PP was added into the chamber of the torque rheometer after PA6/5 wt % organoclay had melted, so PP pellets were surrounded by PA6 phase. After PP pellets had melted, they were stretched into sheets or ribbons and then began to attach to each other. Because of the high volume

TABLE II
Effects of Organoclay Content on the MFI and Equilibrium Torque of PA6/Organoclay

Sample	PA6	PA6/2.5 wt % organoclay	PA6/5 wt % organoclay	PA6/10 wt % organoclay
MFI (g/10 min)	29.4	12.6	5.6	2.3
Equilibrium torque (N·M)	0.5	1.1	1.5	1.8

fraction of PP relative to PA6, there was a tendency to phase inversion. However, phase inversion did not occur due to the barrier effect of organoclay and a three-dimensional network of the PA6 phase turned up [Fig. 4(c1)], being different from that of PA6-30-5md. The three-dimensional network structure of PA6 phase for PA6-30-mi was more resistant to flow induced extension than the two-dimensional network of PA6 phase for PA6-30-5d and PA6-30-5md, and further compounding did not lead to complete destruction of the network [Fig. 4(c2,c3)]. Eventually, the elongated network of PA6 shown in Figure 1(e) was obtained.

Key factors in promoting cocontinuous structure

The viscosity increase of the minor polymer component in which organoclay was selectively distributed and the barrier effect of organoclay were proposed in Refs. 6–10 as possible reasons for the change in final phase morphology from matrix-dispersed to cocontinuous morphology by the incorporation of organoclay. To gain a deep understanding of the effect of organoclay in promoting cocontinuous morphology, verification of the contribution of these two factors was conducted.

Table II summarizes the effect of organoclay content on the viscosity of PA6 expressed in terms of MFI and equilibrium torque. With increasing organoclay loading, the MFI of PA6/organoclay decreases and the equilibrium torque of PA6/organoclay increases obviously. Both the decrease in MFI and in equilibrium torque indicate a significant the increase in the melt viscosity of PA6 as the amount of organoclay increases.

To know whether the increase in viscosity of PA6 is the sole reason for the formation of cocontinuous morphology, a high molecular weight PA6 (HMWPA6) with MFI (2.6 g/10 min) similar to that of PA6/10 wt % organoclay was used to prepare PP/HMWPA6 (70/30, w/w) blend in the absence of organoclay using mi compounding sequence. A typical matrix-dispersed morphology with spherical HMWPA6 particles was obtained [Fig. 5(a)], indicating that solely viscosity increase of the HMWPA6 phase is not sufficient to promote cocontinuous morphology and the barrier effect of organoclay must play an important role.

Next, PP/HMWPA6 (70/30, w/w) blends containing 2.5 and 5 wt % of organoclay were prepared to investigate the effect of the viscosity of PA6 on the formation of cocontinuous morphology. As shown in Figure 5(b,c), cocontinuous morphology was obtained in both cases. With 2.5 wt % of organoclay, a highly elongated network structure of HMWPA6 phase with quite long distance between branched points was obtained, which is quite different from the matrix-dispersed morphology of PA6-30-2.5mi [Fig. 6(a)], indicating that the viscosity increase of PA6 favors the formation of cocontinuous morphology. The network structure of PA6 phase can be seen as a combination of many long threads of

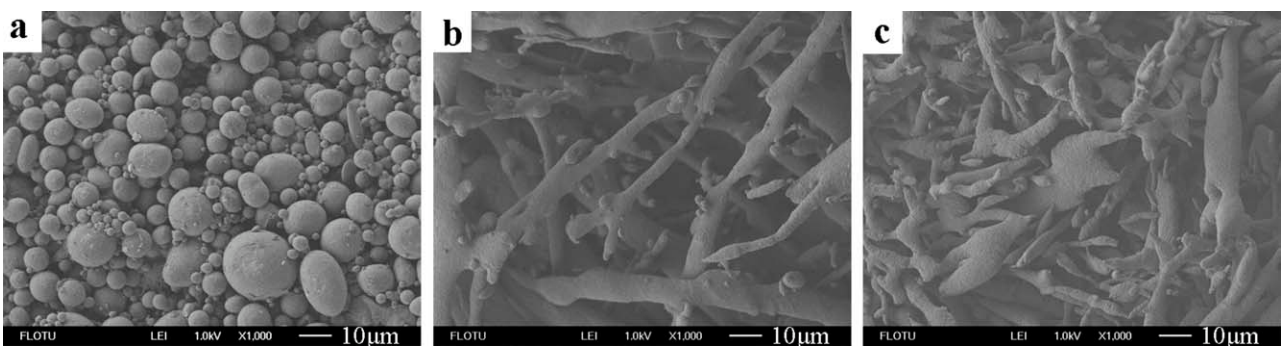

Figure 5 FESEM images of the HMWPA6 phases of PP/HMWPA6 blends containing different amounts of organoclay: (a) 0 (HMWPA6-30-0mi), (b) 2.5 wt % (HMWPA6-30-2.5mi), and (c) 5 wt % (HMWPA6-30-5mi).

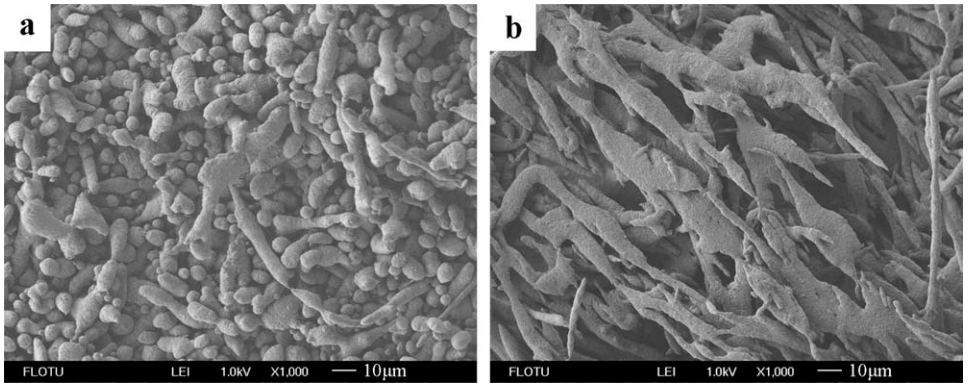

Figure 6 FESEM images of the PA6 phases of PP/PA6 blends containing different amounts of organoclay: (a) 2.5 wt % (PA6-30-2.5mi) and (b) 10 wt % (PA6-30-10mi).

PA6,[36] thus the effect of viscosity can be understandable by considering the stability of a long polymer thread encapsulated in the melt of another polymer. Tomotika[37] has developed a theory of the instability of a liquid cylinder surrounded by another liquid. For sinusoidal capillarity wave instabilities, the breakup time of the liquid cylinder has been estimated to be:

$$t_b = \frac{1}{q} \times \ln\left(\frac{k}{\alpha_0}\right), \tag{2}$$

where $k = 0.8R_0$ and q is defined as

$$q = \left(\frac{\sigma}{2\eta_m R_0}\right)\Omega(\ell, \lambda), \tag{3}$$

where σ = interfacial tension, η_m = matrix viscosity, R_0 = initial thread radius, and Ω (ℓ, λ) is the Tomotika function, which is the dimensionless distortion growth rate of the thread depending upon the distortion wavelength ℓ and the viscosity ratio λ.

Equations 2 and 3 give that a high viscosity ratio (η_d/η_m), low interfacial tension, large initial thread diameter, and relatively high matrix viscosity lead to larger t_b, thus is beneficial to the stabilization of the thread. Considering the equal amount of organoclay in HMWPA6-30-2.5mi and PA6-30-2.5mi, the intensity of the barrier effect of organoclay should be similar for the two samples. The comparatively higher viscosity of HMWPA6 prolonged the breakup time for the fibers constituting the network structure of HMWPA6, thus the fibers were extended to a large aspect ratio without breakup. Consequently, the network structure of HMWPA6 was preserved, with very long distance between branched points.

The analysis above leads to the conclusion that both the viscosity increase of the PA6 phase and the barrier effect of organoclay contribute to the formation of cocontinuous morphology at asymmetric compositions through stabilizing the fibers constituting the network structure of PA6.

Effect of the amount of organoclay

Apart from 5 wt %, other organoclay loadings (2.5 and 10 wt % to PA6) were also used to prepare PP/PA6 blends to investigate the effect of the amount of organoclay on the final phase morphology. As is shown in Figure 6(a), no sign of cocontinuous structure can be detected but many fibrils or rod-like particles were observed, indicating that a critical amount of organoclay is needed to promote cocontinuous phase morphology. When the amount of organoclay is 10 wt % [Fig. 6(b)], cocontinuous type morphology becomes more distinct and coarser compared to PA6-30-5mi. The average fiber diameter constituting the network structure is roughly 6 μm. This indicates that the increase in organoclay loading favors the formation of cocontinuous morphology.

The effect of organoclay loading on phase morphology is completely understandable considering the two key factors in promoting cocontinuous morphology discussed above. A critical amount of organoclay is needed so that the viscosity increase and the barrier effect of organoclay are sufficient to prolong t_b to a length beyond the compounding time. Beyond the critical amount of organoclay, the network structure of PA6 phase formed in the early stage of mixing can be kept to some extent rather than destroyed completely. As the amount of organoclay increases further, the stabilizing effects get intenser so that the deformation ability of the PA6 phase is decreased, resulting in a coarser network of PA6.

More asymmetric blending composition

Attempts were made to check whether cocontinuous morphology could be obtained at a more asymmetric composition (PP/PA6 = 80/20 w/w) by the incorporation of organoclay, and the results are shown in

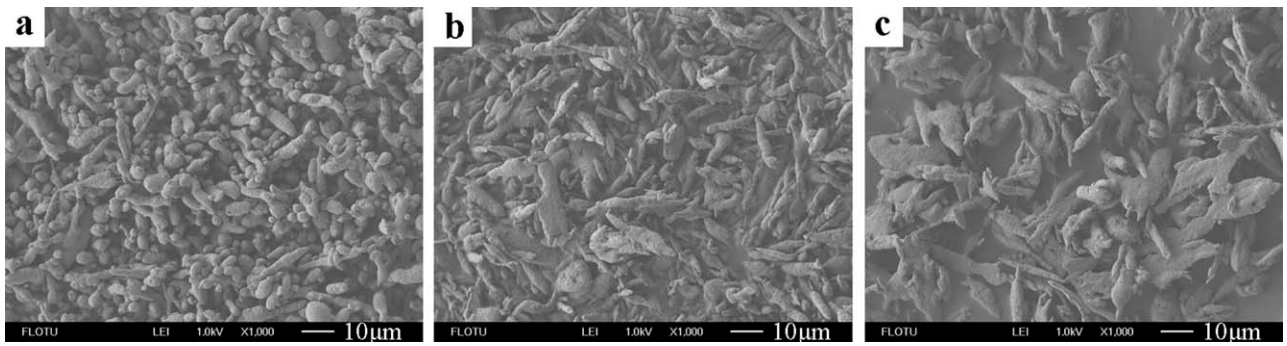

Figure 7 FESEM images of the PA6 phases of PP/PA6 blends at a more asymmetric composition (80/20 w/w) containing different amounts of organoclay: (a) 5 wt % (PA6-20-5mi), (b) 10 wt % (PA6-20-10mi), and (c) 15 wt % (PA6-20-15mi).

Figure 7. For all three organoclay loadings (5, 10, and 15 wt %), matrix-dispersed morphology were obtained, showing the incapability of organoclay in promoting cocontinuous morphology for the PP/PA6 80/20 blend.

For organoclay-filled PP/PA6 80/20 blends, the morphology evolution at the initial stage should be similar to that of PA6-30-5mi. However, due to a lower volume fraction of the PA6 phase (about 17%), the network of PA6 would endure more severe extension by flow field than that for PA6-30-5mi. According to eqs. 2 and 3, smaller initial radius leads to smaller t_b. Thus, the thinner fibers constituting the network of PA6 for PP/PA6 80/20 blends would be easier to break up than those for PA6-30-5mi. Consequently, the network structure of PA6 broke up completely and matrix-dispersed morphology was obtained.

Dynamic mechanical properties

DMA was carried out on the blends containing 5 wt % of organoclay (to PA6) prepared by the three different compounding sequences and on the blend without organoclay as reference. The curves of storage modulus versus temperature are given in Figure 8. The curve of PA6-30-5d lies slightly below that of PA6-30-0d, being similar to the case of PP/PET blend[38] where incorporation of clay by direct melt mixing led to a decrease in storage modulus due to weak adhesion between phases. The storage modulus of PA6-30-5 mi, which has cocontinuous morphology, was the highest among the three organoclay-filled blends. At 25°C, the storage modulus of PA6-30-5mi was nearly 1.58 times of that of PA6-30-5d and 1.15 times of that of PA6-30-md. With decreasing temperature, the storage modulus improvement of PA6-30-5mi compared to PA6-30-5md and PA6-30-5d became larger. This indicates that the reinforcement effect of organoclay is more obvious when it is in the matrix phase, being in agreement with the common knowledge of the morphology-property relations.

CONCLUSIONS

For the asymmetric composition of PP/PA6 70/30, melt mixing PP with premelted PA6/organoclay masterbatch can promote cocontinuous morphology, while direct melt mixing of all the components (PP, PA6, and organoclay) and direct melt mixing of PP with PA6/organoclay masterbatch gave matrix-dispersed morphology. Investigation on the morphology evolution processes of the three different compounding sequences reveals that the main reason for the formation of cocontinuous morphology is the inhibiting effect of organoclay on phase inversion, and consequently the three-dimensional network of PA6 phase formed in the initial stage of the mixing can be kept to some extent.

Both the viscosity increase of the PA6 phase where organoclay selectively located and the barrier effect of organoclay are the key factors for the formation of cocontinuous morphology. A critical amount of organoclay is needed to promote cocontinuous morphology. Fine cocontinuous morphology

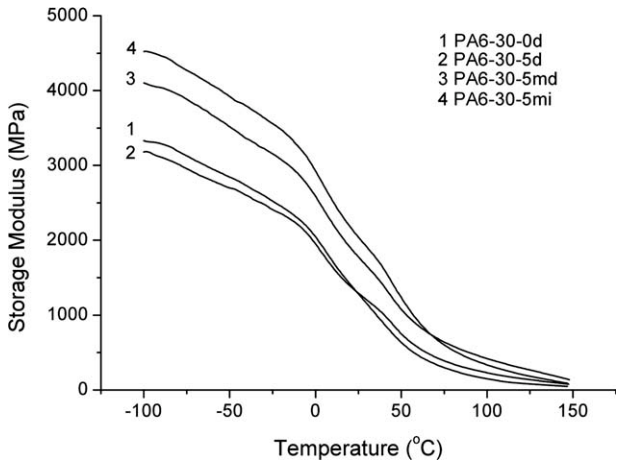

Figure 8 Curves of dynamic storage modulus as a function of temperature for PP/PA6 blend (70/30) without organoclay and those containing 5 wt % organoclay prepared by three different compounding sequences.

can be obtained when the amount of organoclay is 5 wt % (to PA6). With a further increase for organoclay, the cocontinuous morphology becomes much coarser. The incorporation of organoclay fails to promote cocontinuous morphology for PP/PA6 at a more asymmetric composition (80/20 w/w).

DMA shows that the blend having cocontinuous morphology displays increased storage modulus, as compared with pure blend without organoclay and the blends containing the same amount of organoclay but having matrix-dispersed morphology.

References

1. Utracki, L. A. J Rheol 1991, 35, 1615.
2. Zhang, C.; Yi, X. S.; Yui, H.; Asai, S.; Sumita, M. J Appl Polym Sci 1998, 69, 1813.
3. Zou, H.; Wang, K.; Zhang, Q.; Fu, Q. Polymer 2006, 47, 7821.
4. Wu, G. Z.; Li, B. P.; Jiang, J. D. Polymer 2010, 2077, 51.
5. Dhibar, A. K.; Kim, J. K.; Khatua, B. B. J Appl Polym Sci 2011, 119, 3080.
6. Li, Y. J.; Shimizu, H. Polymer 2004, 45, 7381.
7. Wu, D. F.; Zhou, C. X.; Zhang, M. J Appl Polym Sci 2006, 102, 3628.
8. Ray, S. S.; Bandyopadhyay, J.; Bousmina, M. Macromol Mater Eng 2007, 292, 729.
9. Li, Y. J.; Shimizu, H. Macromol Rapid Commun 2005, 26, 710.
10. Filippone, G.; Dintcheva, N. T.; Acierno, D.; Mantia, F. P. L. Polymer 2008, 49, 1312.
11. Zou, H.; Ning, N. Y.; Su, R.; Zhang, Q.; Fu, Q. J Appl Polym Sci 2007, 106, 2238.
12. Filippone, G.; Dintcheva, N. T.; Mantia, F. P. L.; Acierno, D. Polymer 2010, 51, 3956.
13. Filippone, G.; Acierno, D. AIP Conf Proc 2010, 1255, 190.
14. Dintcheva, N. T.; Filippone, G.; Mantia, F. P. L.; Acierno, D. Polym Degrad Stab 2010, 95, 527.
15. Li, B.; Zhang, Y.; Wang, S.; Ji, J. L. Eur Polym Mater 2009, 45, 2202.
16. Wang, Y.; Zhang, Q.; Fu, Q. Macromol Rapid Commun 2003, 24, 231.
17. Khatua, B. B.; Lee, D. J.; Kim, H. Y.; Kim, J. K. Macromolecules 2004, 37, 2454.
18. Ray, S. S.; Bousmina, M. Macromol Rapid Commun 2005, 26, 450.
19. Yoo, Y.; Cui, L. L.; Yoon, P. J.; Paul, D. R. Macromolecules 2010, 43, 615.
20. González, I.; Eguiazábal, J. I.; Nazábal, J. Compos Sci Technol 2006, 66, 1833.
21. Kontopoulou, M.; Liu, Y. Q.; Austin, J. R.; Parent, J. S. Polymer 2007, 48, 4520.
22. Ray, S. S.; Pouliot, S.; Bousmina, M.; Utracki, L. A. Polymer 2004, 45, 8403.
23. Ray, S. S.; Bousmina, M.; Maazouz, A. Polym Eng Sci 2006, 46, 1121.
24. Ray, S. S.; Bousmina, M. Macromol Rapid Commun 2005, 26, 1639.
25. Gcwabaza, T.; Ray, S. S.; Focke, W. W.; Maity, A. Eur Polym Mater 2009, 45, 353.
26. Tang, Y.; Hu, Y.; Zhang, R.; Gui, Z.; Wang, Z. Z.; Chen, Z. Y.; Fan, W. C. Polymer 2004, 45, 5317.
27. Feng, M.; Gong, F. L.; Zhao, C. G.; Chen, G. M.; Zhang, S. M.; Zhang, S. M.; Yang, M. S.; Han, C. C. J Polym Sci Part B: Polym Phys 2004, 42, 3428.
28. Feng, M.; Gong, F. L.; Zhao, C. G.; Chen, G. M.; Zhang, S. M.; Zhang, S. M.; Yang, M. S. Polym Int 2004, 53, 1529.
29. Gahleitner, M.; Kretzschmar, B.; Pospiech, D.; Ingolic, E.; Reichelt, N.; Bernreitner, K. J Appl Polym Sci 2006, 100, 283.
30. Gahleitner, M.; Kretzschmar, B.; Vliet, G. V.; Devaux, J.; Pospiech, D.; Bernreitner, K.; Ingolic, E. Rheol Acta 2006, 45, 322.
31. Shim, J. H.; Joo, J. H.; Jung, S. H.; Yoon, J. S. J Polym Sci Part B: Polym Phys 2007, 45, 607.
32. Letuchi, M.; Tzur, A.; Tchoudakov, R.; Narkis, M.; Siegmann, A. Polym Compos 2007, 28, 417.
33. Su, Q. S.; Feng, M.; Zhang, S. M.; Jiang, J. M.; Yang, M. S. Polym Int 2007, 56, 50.
34. Pötschke, P.; Paul, D. R. Macromol Symp 2003, 198, 69.
35. Scott, C. E.; Macosko, C. W. Polym Bull 1991, 26, 341.
36. Pötschke, P.; Paul, D. R. J Macromol Sci Polym Rev 2003, C43, 87.
37. Tomotika, S. Proc R Soc London 1935, 150, 322.
38. Calcagno, C. I. W.; Mariani, C. M.; Teixeira, S. R.; Mauler, R. S. Compos Sci Technol 2008, 68, 2193.